MECHANICAL PROPERTIES OF COAL MEASURE ROCKS CONTAINING FLUIDS AT PRESSURE

Ian Gray[1], Xiaoli Zhao[2], Lucy Liu[3]

ABSTRACT: The sedimentary rock that comprises coal measures has quite nonlinear, elastic, stress – strain characteristics. It is also affected by the fluid pressure within it. The fluids act in two quite separate ways. The first way in which fluid acts is in a poroelastic manner while the second is within fractures. These effects are important in rock behaviour, extending from the deformation around a roadway to failure within an outburst. This paper presents the results of detailed laboratory studies into coal and sedimentary rock properties. It relates these to the real situations seen in mining.

1. **INTRODUCTION**

All sedimentary rocks exhibit variability in both Young's moduli and Poisson's ratios under different stresses. Some are also quite anisotropic. This nonlinear, anisotropic, elastic behaviour is extremely important in determining the stresses within the rock mass both in the virgin state and as a response to mining. Fluid pressure within the rock mass is also important as it is a component of effective stress.

Determining these rock properties is quite complex. The options are uniaxial testing, triaxial testing and hydrostatic testing. The usual procedure is to rely on simple uniaxial testing. This however tends to give quite inadequate results. Uniaxial testing only enables the axial modulus to be determined over a very limited stress range before the sample starts to fail. This failure is accompanied by a rapid increase in Poisson's ratio. The single measurable value of Poisson's ratio cannot therefore be gauged accurately. It is also impossible to subject a uniaxial sample to the effects of fluid pressure.

Triaxial testing permits the Young's modulus and Poisson's ratios to be determined by axial and radial (confining stress) loading of a strain gauged core sample in a triaxial cell. The core is loaded sequentially with changes in axial and then radial pressure to enable the determination of the Young's moduli and Poisson's ratios. Mathematics has been developed to determine these values on the basis that the rock behaves as an orthotropic material. This form of triaxial testing is not the same as that used to determine the ultimate strength parameters of the rock.

Hydrostatic testing is suitable to measure the behaviour of rock fragments. This is especially common in coal. This method involves strain gauging a fragment with multiple rosettes, casting in a soft resin, and then hydrostatically loading it while recording the strain behaviours.

Figure 1 shows examples of these three test methods. The leftmost photograph in Figure 1 shows all of the problems of dealing with a piece of weak disintegrating coal core in uniaxial testing. The sample is too short, it is dimensionally uneven and the ends cannot be cut parallel and have to be built up with plaster. The test is slightly better than useless for determining material properties.The middle photo shows a similar coal sample that has been fitted with strain gauges and is contained in silicone resin prior to hydrostatic testing. The rightmost photo shows a good core of a stronger coal that is ready to triaxially tested.

---

1) Managing Director, Sigra Pty Ltd ian@sigra.com.au Tel +61 7 3216 6344
2) Reservoir Engineer, Sigra Pty Ltd, xiaoli@sigra.com.au
3) Laboratory Technician Sigra Pty Ltd lucy@sigra.com.au

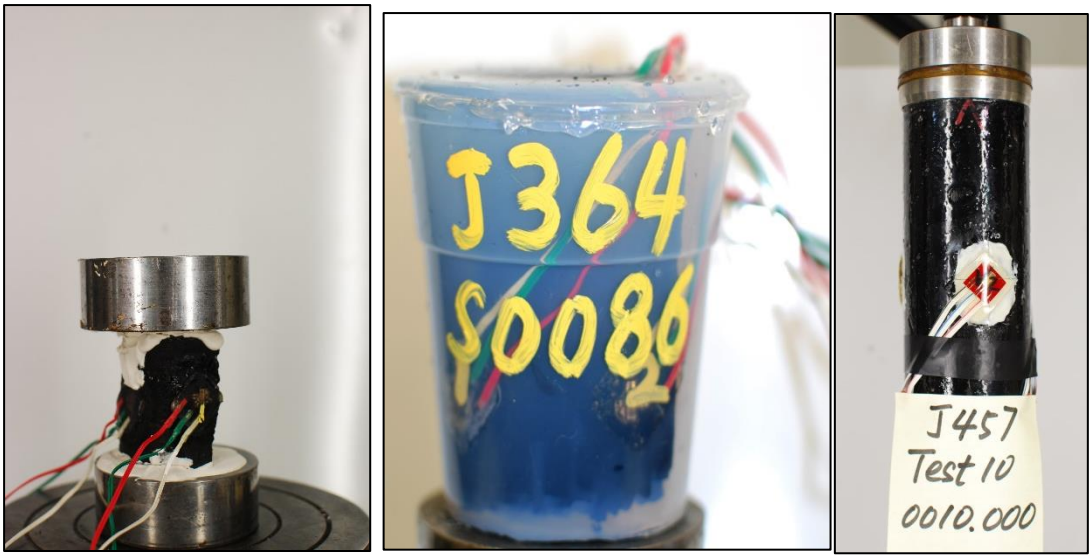

Figure 1. Coal sample for uniaxial test (left), and coal fragment for hydrostatic test (middle), and triaxial test (right).

2. STRESS STRAIN RELATIONSHIPS

A solid may be subject to six stresses which produces six strains. The relationship between stress and strain therefore contains 36 components. Determining all of these is practically impossible. However if the assumption is made that the rock is orthotropic this can be simplified to twelve unknowns. If one of the axes of symmetry can be identified, such as that perpendicular to a bedding plane, this is reduced to nine as shown in Equation (1) which relates principal stresses and strains. The symmetry of this matrix means that the relationship of Equation (2) applies.

$$\begin{bmatrix}\Delta\varepsilon_{11}\\ \Delta\varepsilon_{22}\\ \Delta\varepsilon_{33}\end{bmatrix}=\begin{bmatrix}\frac{1}{E_1} & -\frac{\nu_{21}}{E_2} & -\frac{\nu_{31}}{E_3}\\ -\frac{\nu_{12}}{E_1} & \frac{1}{E_2} & -\frac{\nu_{32}}{E_3}\\ -\frac{\nu_{13}}{E_1} & -\frac{\nu_{23}}{E_2} & \frac{1}{E_3}\end{bmatrix}\begin{bmatrix}\Delta\sigma_{11}\\ \Delta\sigma_{22}\\ \Delta\sigma_{33}\end{bmatrix} \quad (1)$$

$$\frac{\nu_{ij}}{E_i}=\frac{\nu_{ji}}{E_j} \quad (2)$$

The term ν_{ij} refers to the Poisson's ratio associated with dilation in the *j* direction brought about by loading in the *i* direction.

These two relationships mean that there are six unknowns to be solved. Given two potential loading cases – axial and radial, and three radial strains, this set of equations cannot be solved for Young's moduli and Poisson's ratios. Making the assumption of Equation 3 that introduces the concept of a geometric mean value of Poisson's ratio makes it possible to solve all values of Young's modulus and Poisson's ratio.

$$\nu_a^2=\nu_{ij}\nu_{ji}=\nu_{jk}\nu_{kj}=\nu_{ik}\nu_{ki} \quad (3)$$

By manipulation of these equations the solution for Young's modulus can be described by Equation 4 which can be fully solved in the case of axial and radial loading steps. This is achieved by a nonlinear solution process in which the value of ν_a is adjusted to provide a best fit between the axial modulus derived from radial loading and that derived from axial loading.

$$E_i=\frac{1}{\Delta\varepsilon_i}\left(\Delta\sigma_i-\sqrt{\frac{E_i}{E_j}}\nu_a\Delta\sigma_j-\sqrt{\frac{E_i}{E_k}}\nu_a\Delta\sigma_k\right) \quad (4)$$

In hydrostatic test no solution to the value of v_a can be obtained from the test process and v_a has to be estimated. Using this estimated value of v_a the values of Young's moduli and Poisson's ratios can be derived using Equation 5.

$$E_i = \frac{\Delta\sigma}{\Delta\varepsilon_i}\left(1 - \sqrt{\frac{E_i}{E_j}}v_a - \sqrt{\frac{E_i}{E_k}}v_a\right) \quad (5)$$

Effect of fluid pressure

Fluid pressure operates on open spaces within the rock mass. A fluid pressure change may lead to a deformation of the rock mass which then behaves as though it were a change in stress. It may also act directly on open spaces or fractures changing the normal stress within these. Either of these effects may be described by Equation 5 (Gray et al, 2017).

$$\sigma'_{ij} = \sigma_{ij} - \delta_{ij}\alpha_i P \quad (6)$$

Where: σ'_{ij} is the effective stress on a plane perpendicular to the vector *i* in the direction *j*.
σ_{ij} is the total stress on a plane perpendicular to the vector *i* in the direction *j*.
δ_{ij} is the Kronecker delta. If $i \neq j$ then $\delta_{ij} = 0$, while if $i = j$ then $\delta_{ij} = 1$.
α_i is a poroelastic coefficient affecting the plane perpendicular to the vector *i*. Its value lies between 0 and 1.
P is the fluid pressure in pores and fractures within the rock.

In the poroelastic case Equation 1 can be re-written using Equation 6 as Equation 7.

$$\begin{bmatrix}\Delta\varepsilon_{11}\\ \Delta\varepsilon_{22}\\ \Delta\varepsilon_{33}\end{bmatrix} = \begin{bmatrix}\frac{1}{E_1} & -\frac{\nu_{21}}{E_2} & -\frac{\nu_{31}}{E_3}\\ -\frac{\nu_{12}}{E_1} & \frac{1}{E_2} & -\frac{\nu_{32}}{E_3}\\ -\frac{\nu_{13}}{E_1} & -\frac{\nu_{23}}{E_2} & \frac{1}{E_3}\end{bmatrix}\begin{bmatrix}\Delta\sigma_{11}\\ \Delta\sigma_{22}\\ \Delta\sigma_{33}\end{bmatrix} - \Delta P\begin{bmatrix}\frac{1}{E_1} & -\frac{\nu_{21}}{E_2} & -\frac{\nu_{31}}{E_3}\\ -\frac{\nu_{12}}{E_1} & \frac{1}{E_2} & -\frac{\nu_{32}}{E_3}\\ -\frac{\nu_{13}}{E_1} & -\frac{\nu_{23}}{E_2} & \frac{1}{E_3}\end{bmatrix}\begin{bmatrix}\alpha_1\\ \alpha_2\\ \alpha_3\end{bmatrix} \quad (7)$$

Equation 7 describes the deformation of rock due to changes in stress and fluid pressure. The poroelastic coefficients (α_i) lie between zero and unity.

It is possible to solve Equation 7 in the triaxial testing by axial and radial loading stages and by introducing fluid injection. $E_1, \nu_{12}\ and\ \nu_{13}$ are determined from axial loading, and $E_2,\ E_3,\ \nu_{21}, \nu_{31}, \nu_{23}, \nu_{32}$ are deduced through the radial loading step . The strain changes associated with fluid injection may be measured and provide sufficient information to derive a solution for the poroelastic coefficients.

If a rock mass contains an open joint then the effect of fluid pressure acting within it may be better described by Equation 6 alone where α_i may be thought of as the ratio of open fracture to total area. In reality the rock mass will never contain a totally open joint and some poroelastic effect will be present; the values of α_i may be expected to vary as the joint opens and closes.

It should be appreciated that in typical sedimentary rock with nonlinear characteristics the values of all Young's moduli, Poisson's ratios and the poroelastic coefficients vary with the state of stress.

3. EXPERIMENTAL PROCEDURES

Uniaxial testing may follow a standard such as AS 4133.4.3.1 – 2009. However, proper attention to the testing process and analysis process is required. The stress and strain values obtained from a uniaxial cyclic loading test are shown in Figure 2. The sample is a typical sandstone and the results of the test are extremely non-linear. This non-linearity is generally ignored and the results are quoted in terms of a tangent and secant modulus at 50% of ultimate strength. This ignores the fact that the

tangent modulus frequently increases four fold before it begins to decline with the onset of failure. This onset of failure is frequently associated with the value of tangent modulus exceeding 0.5.

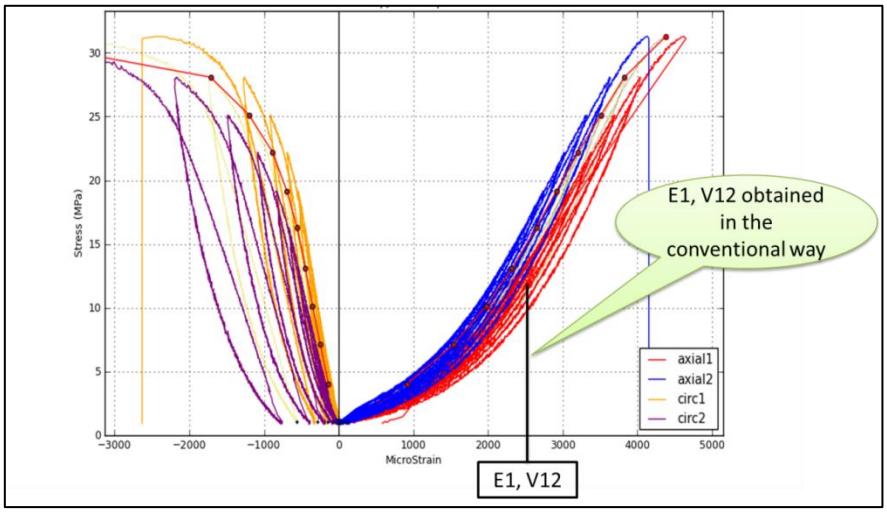

Figure 2. Uniaxial test – stress versus strain plot.

Triaxial testing is conducted on core sample fitted with three rosettes disposed at 120 degrees around the circumference. Typically four loading tests are conducted. The test sequence is first to load in relatively equal stages of axial and radial (confining) stress so as to avoid causing the sample to fail. The sample is then unloaded in a similar manner. A second stage involves loading but with a lower confining stress – typically 80% of axial. This procedure is then repeated with radial stress at 60%, 40% and 25% of axial before testing with axial stress alone. This procedure minimises the risk of the sample failing early in the process through excessive shear stress. In addition to the axial and radial loading cycles, fluid, usually nitrogen or helium, is injected into the rock between direct loading cycles to enable the determination of poroelastic behaviour.

Figure 3 shows the loading cycle where the radial stress is 80% of axial stress. This test also includes the injection of nitrogen into the sample.

The hydrostatic test involves fitting strain gauges to the sample. These may be rosettes placed on orthogonal faces or a rosette on a bedding plane and single gauges perpendicular to the bedding plane. The fragment is then set in silicone resin, hydrostatically loaded, and the strain monitored as shown in Figure 4. This is usually conducted in a cyclic loading process so that the loading and unloading Young's moduli may be determined.

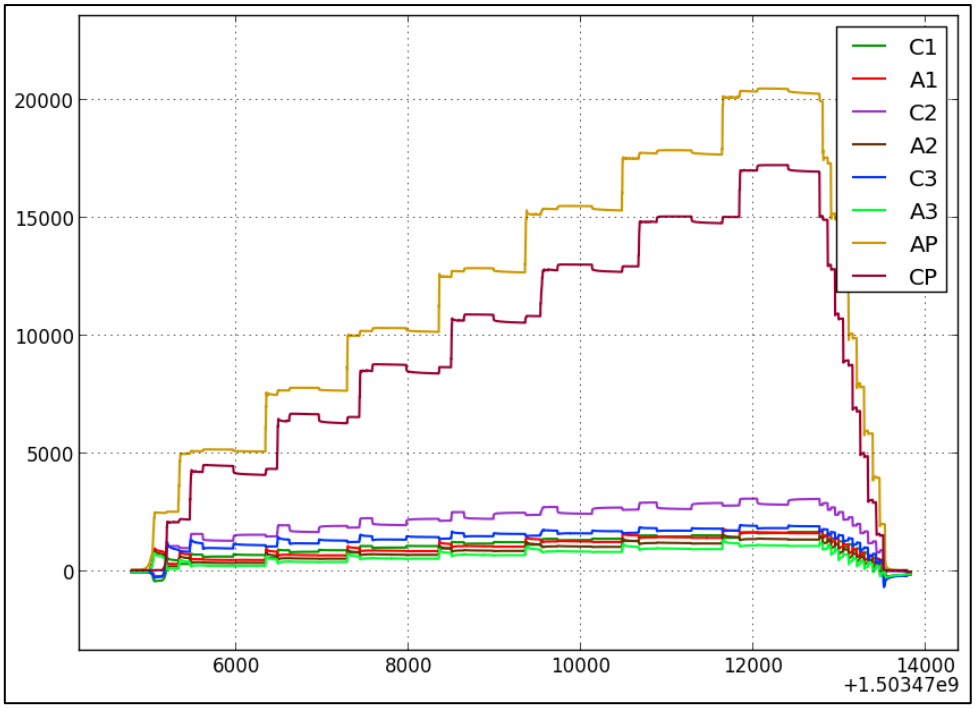

Figure 3. Triaxial test to determine Young's moduli, Poisson's ratios and the poroelastic coefficient. X axis time (s), Y axis stress (AP and CP in kPa), and microstrain.

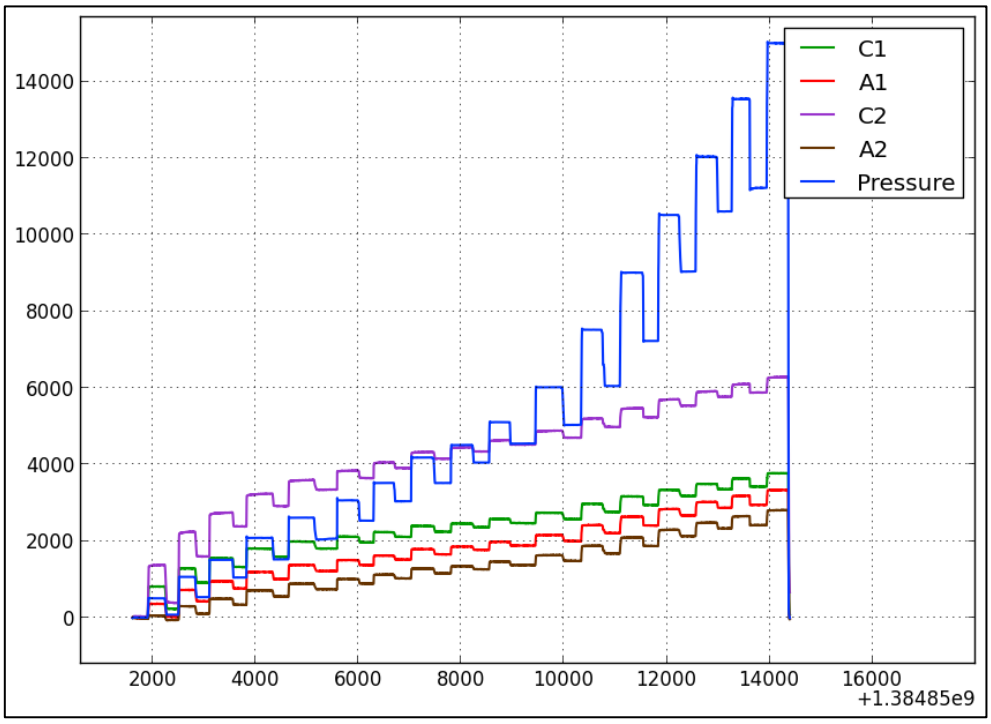

Figure 4. Hydrostatic test. X axis time (s), Y axis pressure (kPa) and microstrain.

4. EXPERIMENTAL RESULTS

A coal sample from the Goonyella Middle (GM) seam in Bowen basin has been tested both uniaxially and hydrostatically. Coal samples from the Bulli seam in the Sydney Basin and a porous Hawkesbury sandstone sample from Sydney have been tested triaxially.

4.1. Uniaxial test results

The results from non-cyclic uniaxial testing a sample from the GM seam are shown in Figure 5. The GM seam sample was of similar poor form as that shown in the left hand photo of Figure 1. The sample's stiffness changes during the test with a general tendency to increase but with obvious stages of failure. The right side of Figure 5 shows Poisson's ratio, which suddenly increases as failure approaches.

The sample is clearly nonlinear in its behaviour and yet conventional reporting would typically provide a single value based on a fixed percentage (usually 50%) of the ultimate stress. Figure 5 indicates that the secant Young's moduli and Poisson's ratios vary over two fold over the range of the test. The tangent Young's moduli fluctuate greatly and vary over four fold over the test. The tangent Poisson's ratio increases significantly with stress. When stress approaches 8 MPa, the value of Poisson's ratio reaches 0.5, meaning that the sample is behaving plastically at this stress level. At stresses above this level the sample is dilating. This behaviour is quite normal for coal under uniaxial testing. Better samples of sandstone or siltstone will give smoother change in tangent modulus and a gradually increasing Poisson's ratio.

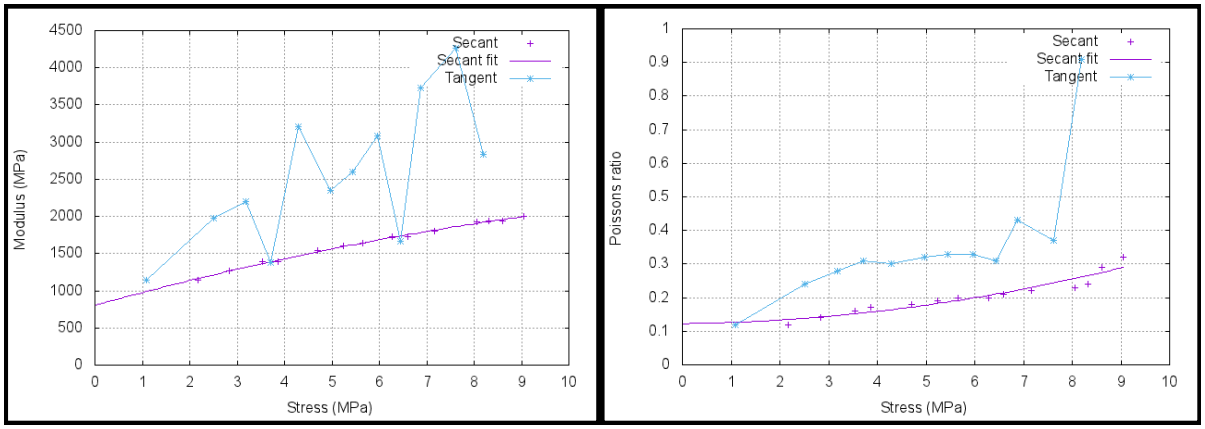

Figure 5. Results from uniaxial test – Young's modulus (left) and Poisson's ratio (right)

4.2 Hydrostatic test results

Figure 6 shows the result of a hydrostatic test of the GM seam coal sample. The secant Poisson's ratio for the uniaxial test ranges between 0.1 and 0.3 and a value of a geometric mean Poisson's ratio v_a of 0.2 is used in the analysis of the hydrostatic testing. The sample is obviously nonlinear and anisotropic. The axial Young's modulus is the lowest among all the values, being 500-1000 MPa lower than the minor transverse Young's modulus. It is 2000 MPa less than that of the major. The sample is nonlinearly elastic with the values of three Young's moduli varying two to more than three fold over the range of the test.

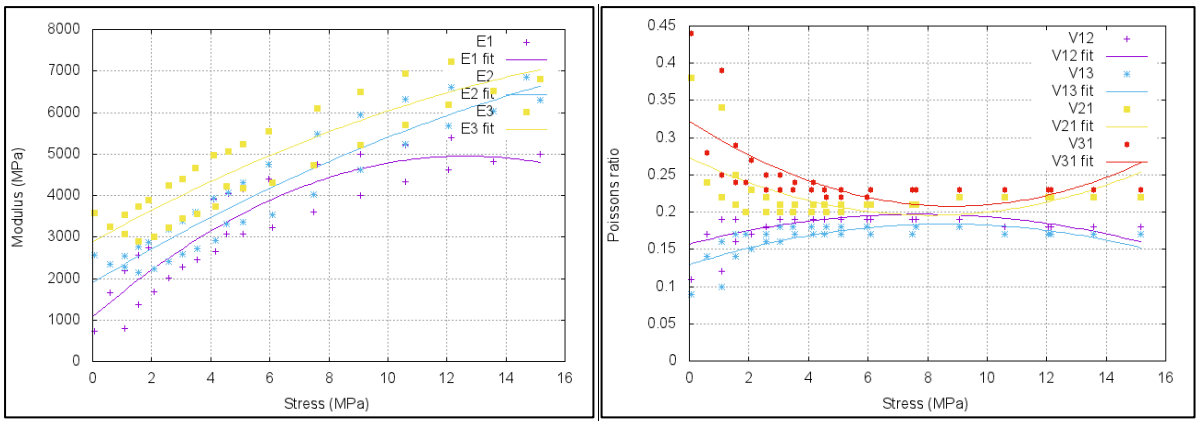

Figure 6. Hydrostatic results – Young's modulus (left) and Poisson's ratio (right) plotted with respect to hydrostatic stress. The assumption used in analysis is that v_a=0.2.

4.3 Triaxial elastic test results

Figure 7 shows the axial Young's modulus of a dull Bulli coal sample plotted against axial and confining stress. Figure 8 shows the major transverse Young's modulus which is similar in value to the axial modulus. Both moduli show a large increase in value with stress. The axial modulus is dependent on both axial and confining with axial stress having a slightly more dominant effect. The major transverse modulus appears to be slightly more dependent on confining stress.

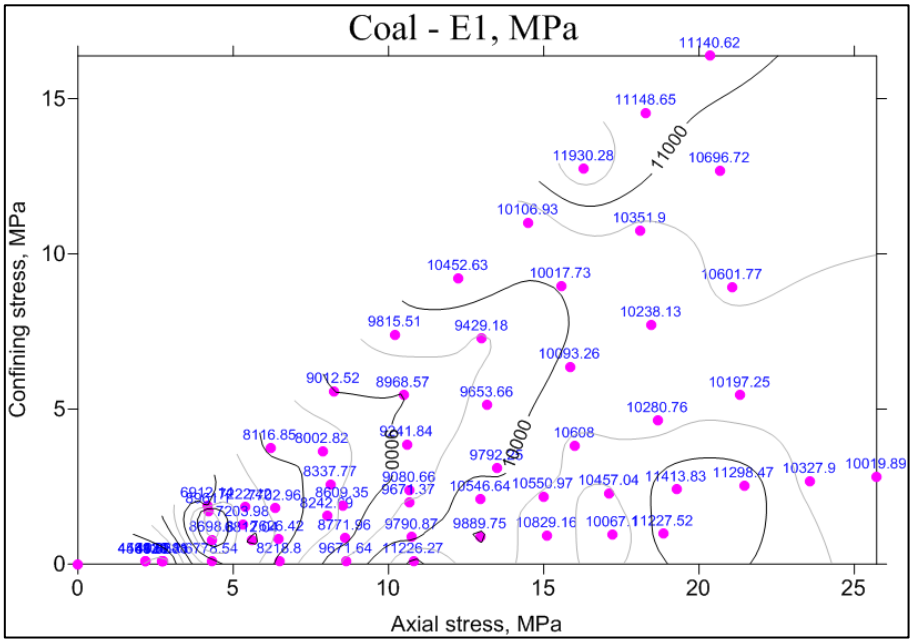

Figure 7. Axial Young's modulus (E_1) of coal plotted as an isopach with respect to axial and confining stress.

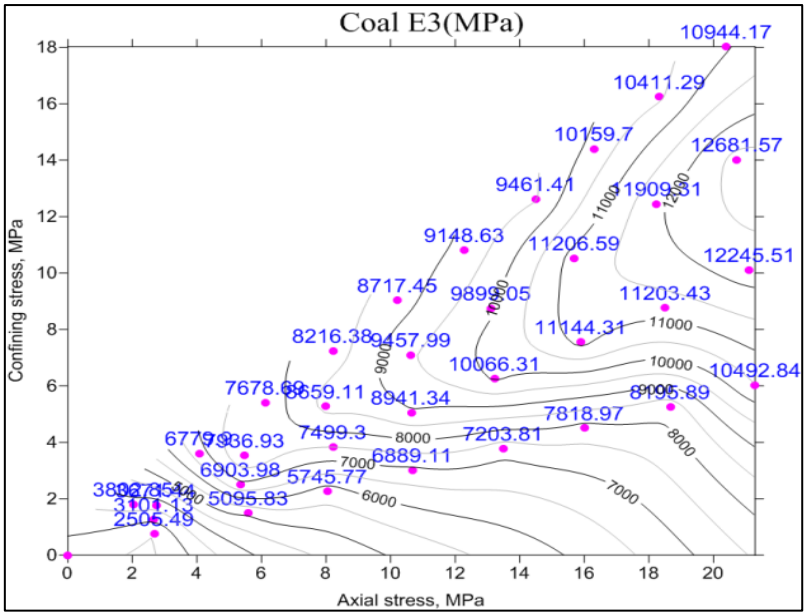

Figure 8. Major transverse Young's modulus of coal(left) and porous sandstone (right) plotted as an isopach on axial and confining stress.

The second sample is a porous medium grained Hawkesbury sandstone which has been cored approximately perpendicular to the bedding plane. The left picture in Figure 9 shows the axial Young's modulus (E_1), which is perpendicular to the bedding plane, plotted with respect to axial and confining stress. E_1 increases with stress and is primarily a function of the axial stress. The major transverse Young's modulus shown in the right picture in Figure 9 also stiffens with stress but is primarily a function of the confining stress. In this sample therefore the value of Young's modulus appears to be controlled by stress in the direction of the modulus being determined.

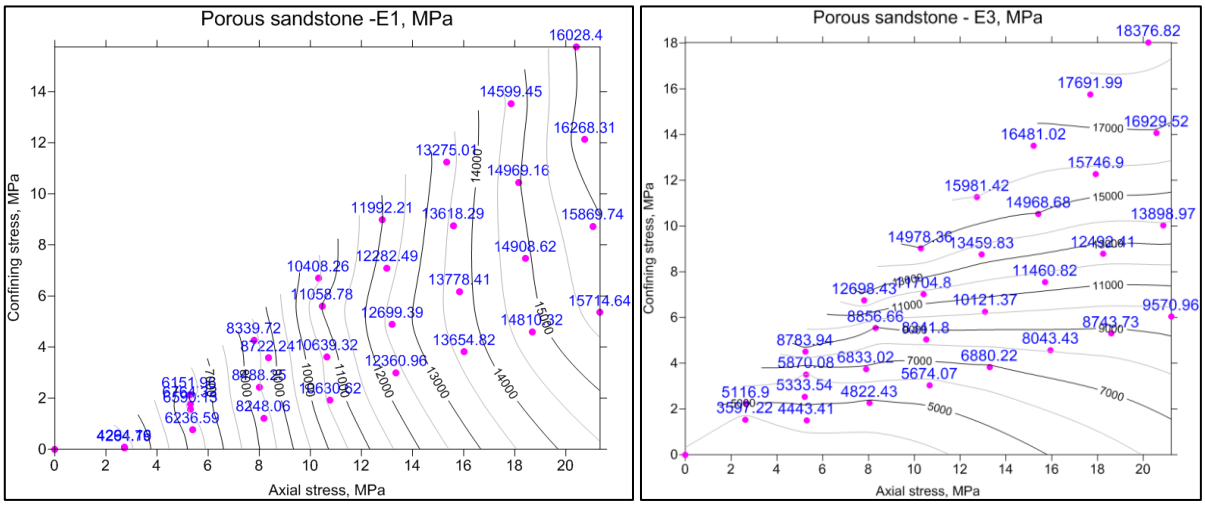

Figure 9. Axial(E_1) and major transverse Young's modulus of porous sandstone plotted as an isopach with respect to axial and confining stress.

Not all sandstone samples behave in this way. Some have shown values of Young's moduli that are a function of axial and confining stress.

Figure 10 shows the trend of geometric mean Poisson's ratio (ν_a) for the coal sample (left) and the porous sandstone (right). The values of ν_a in the coal vary little, but are quite dependent on the shear stress in the porous sandstone. The latter trend is more frequently observed.

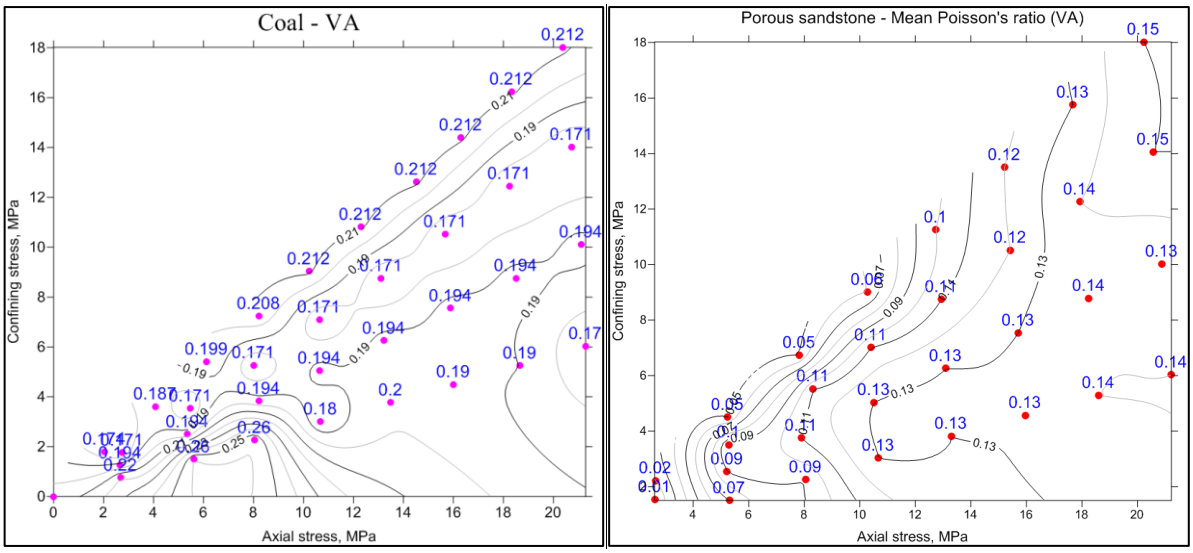

Figure 10. Isopachs of the geometric mean Poisson's ratio (ν_a) of coal (left) and porous sandstone (right) plotted between axes of axial and confining stresses

Figure 11 shows the values of Young's modulus determined perpendicular to the bedding plane for a wide number of coals plotted against mean stress. The general trend is for modulus to increase with stress typically four fold, but in some cases ten fold. The more dramatic changes in stiffness are associated with softer coals which tend to be weaker and contain more structure.

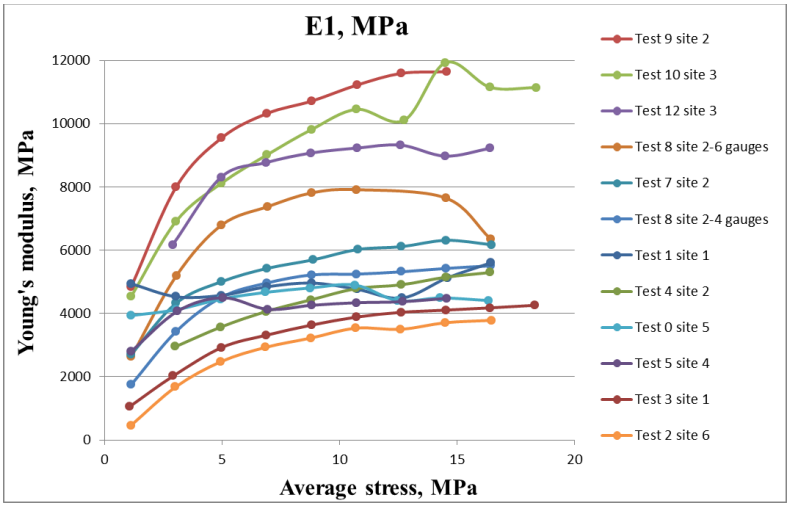

Figure 11. Axial Young's modulus for a variety of coals plotted against mean stress from triaxial testing.

4.3 Poroelastic test results

The poroelastic coefficient describes how the rock or coal deforms with internal fluid pressure as described in Equation 7. The effective stress may be derived from Equation 6. This value of effective stress does not describe the stress at a granular level.

Figure 12 shows the axial poroelastic coefficient of coal and sandstone in the direction of the axis of the samples. The value of the poroelastic coefficient in coal is much lower than that in the porous sandstone. Both values tend to increase with shear stress and decrease with confining stress though to quite different extents.

Extensive tests have shown that the poroelastic coefficient usually lies between 0 to 0.9 in rock, and 0.1 to 0.3 in coal. In coal it tends to be more dependent on the state of stress than in rock.

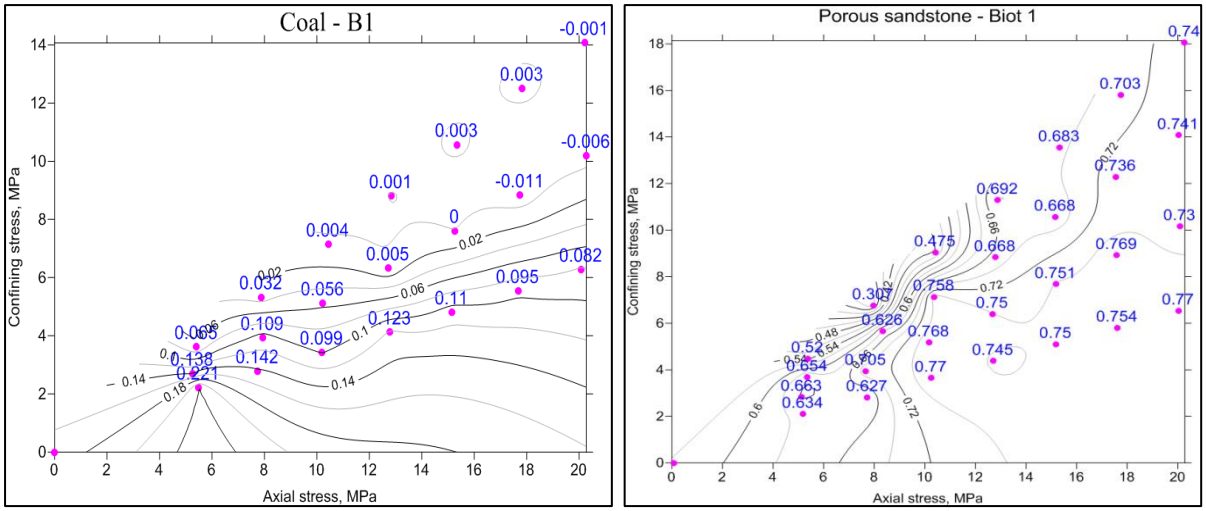

Figure 12. Isopachs of Biot's coefficient for coal (left) and porous sandstone plotted between axes of axial and confining stresses.

5. CONCLUSIONS

This paper compares the mathematics and experimental procedures to obtain orthotropic elastic parameters including poroelastic behaviour using uniaxial, triaxial and hydrostatic testing of coal and sandstone.

Results from the three types of tests show that the mechanical properties of rock vary with stress and may be anisotropic. The effects of fluid pressure within the rock may also be important. Virtually all Young's moduli increase with stress. This variation may be up to ten fold in weaker coals but is frequently four fold. Anisotropy has not been found to be great, usually being less than 1.5:1.

This work highlights the inadequacy of the linear elastic models which ignore fluid pressure and are the basis for the majority of rock mechanic designs at the moment. These simplifications for numerical convenience are significantly in error.

The stiffness of some coals is extremely important in the way in which it may store strain energy. Under the same strain conditions stiffer coals will develop far more stress and higher strain energies. This has important consequences for coalbursting.

The increase in poroelastic coefficient with shear is of importance too as it provides a means by which fluid pressures may act within the coal or rock mass leading to failure. This is as important to outbursting as it is to slope stability.

5. ACKNOWLEDGEMENTS

Some of the work described in this paper has been funded through the Australian Coal Industry Research Program through Project C26061**.**

6. REFERENCES

AS 4133.4.3.1 2009. Methods of testing rocks for engineering purposes Method 4.3.1: Rock strength tests— Determination of deformability of rock materials in uniaxial compression—Strengths of 50 MPa and greater. Standards Australia.

Gray I 2017. Effective Stress In Rock. Deep Mining 2017: Eighth International Conference on Deep and High Stress Mining – J Wesseloo (ed.) © 2017 Australian Centre for Geomechanics, Perth, ISBN 978-0-9924810-6-3